

# Efficient second-harmonic generation from polarized thulium-doped fiber laser with periodically poled MgO:LiNbO<sub>3</sub>

Baofu Zhang, Zhongxing Jiao\*, Biao Wang\*,<sup>1</sup>

State Key Laboratory of Optoelectronic Materials and Technologies, School of Physics and Engineering, Sun Yat-sen University, Guangzhou 510275, China

## ARTICLE INFO

### Article history:

Received 11 October 2014

Received in revised form

25 November 2014

Accepted 14 December 2014

Available online 5 January 2015

### Keywords:

Thulium-doped fiber laser

Second-harmonic generation

High efficiency

## ABSTRACT

We present an efficient method for polarized 963 nm emission based on second-harmonic generation from a high-power, polarized thulium-doped fiber laser using periodically poled MgO:LiNbO<sub>3</sub> as the nonlinear material. The maximum 963-nm output power of 710 mW has been achieved with a pulse duration of 34 ns at the repetition rate of 100 kHz and a Gaussian spatial beam profile. The frequency doubling efficiency is up to 56%, and the total optic-to-optic conversion efficiency is more than 12.9%. In addition, third- and fourth-harmonic generations have been observed.

© 2014 Elsevier Ltd. All rights reserved.

## 1. Introduction

High-power, compact, and efficient laser sources in the near-infrared wavelength region (900–970 nm) are of practical interest in fields such as sensing of water vapor in the atmosphere [1], high-resolution spectroscopy [2], frequency doubling to blue wavelength for applications in data storage and gratings record [3,4]. However, this wavelength region can hardly be directly obtained by conventional laser sources. Operation below ~970 nm cannot be achieved by ytterbium lasers [5]; generation in 910 nm region in the neodymium laser is a three-level transition, and its conversion efficiency can be strongly reduced caused by the parasitic lasing in 1060 nm region [6,7].

Frequency doubling of a thulium-doped fiber laser (TDFL) is an attractive alternative for 900–970 nm generation. TDFLs with their potential broad emission bandwidth (1860–2050 nm) [8] offer distinct superiorities compared to solid-state lasers, including compact size, reduced thermal effects and good beam quality. High-power, pulsed TDFLs have been demonstrated by several groups [9–12]; such systems with high peak power can meet the requirement for second-harmonic generation (SHG). Moreover, efficient frequency doubling can be provided by quasi-phase-matched (QPM) materials, such as periodically poled MgO:LiNbO<sub>3</sub> (MgO:PPLN), attributed to their large nonlinear coefficients combined with reduced walk-off effects [13]. An efficient approach for 9XX nm generation can be

achieved by combining these two mature techniques. By frequency doubling of a TDFL, Frith et al. have obtained about 60% conversion efficiency of the pulsed 1908 nm source, with about 800 mW average power at 954 nm [14]. However, the master oscillator (MO) in their TDFL system did not produce linearly polarized output, and hence the large launch loss through a polarization-sensitive isolator led to small launched power into the power amplifier (PA). Furthermore, small MO seed power and strong reabsorption in the thulium fiber would result in low polarization extinction ratio (PER) of the PA output power; only a beam in appropriate polarization orientation was useful in SHG, and therefore the total optic-to-optic conversion efficiency in this system was restricted.

In order to improve the total optic-to-optic conversion efficiency of SHG from TDFL, a high-power linearly polarized seed source is necessary; our approach is to scale the output power of an all-fiber, polarized, thulium-doped MOPA system which is reported in our previous work [12]. In this paper, an efficient SHG from polarized TDFL system based on MgO:PPLN is presented; a theoretical model is also employed. With the optimal operating temperature of the MgO:PPLN, we have achieved 963 nm output power of 710 mW, with up to 56% frequency doubling efficiency and total optic-to-optic conversion efficiency more than 12.9%. These results are consistent with the theoretical model we performed. In addition, third- and fourth-harmonic generations have been observed.

## 2. Experiment

The experiment configuration consists of three subsystems: a TDFL seed source, a stage of amplification at fundamental wavelength and a

\* Corresponding authors.

E-mail addresses: [jiaozhx@mail.sysu.edu.cn](mailto:jiaozhx@mail.sysu.edu.cn) (Z. Jiao), [wangbiao@mail.sysu.edu.cn](mailto:wangbiao@mail.sysu.edu.cn) (B. Wang).

<sup>1</sup> Tel.: +86 2084115692.

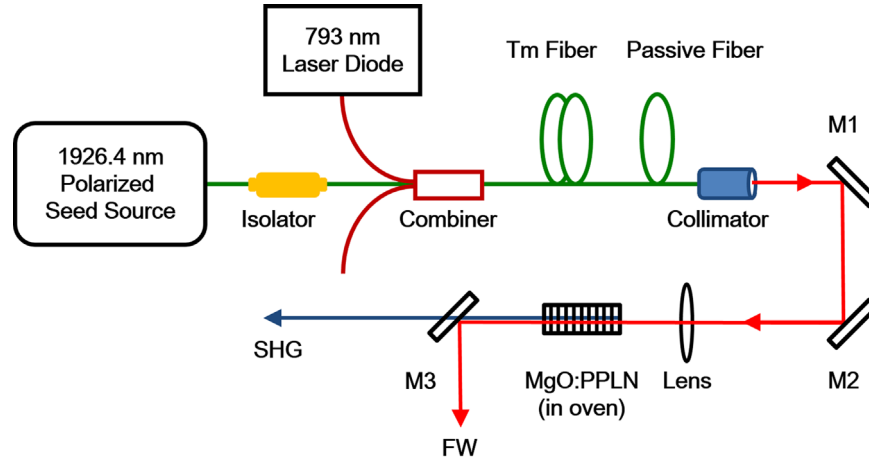


Fig. 1. The scheme of the amplification stage of the thulium-doped fiber seed source and second-harmonic generation experiment based on MgO:PPLN.

SHG stage based on MgO:PPLN ( $e+e \rightarrow e$ ). The schematic of our experimental setup is depicted in Fig. 1.

The seed power for the amplification stage was produced by an all-fiber 1550-nm-pumped polarized thulium-doped MOPA system [12]. The high peak power and the linear polarization of this seed source enable efficient power amplification to a sufficient level for frequency doubling.

The seed laser was launched into the PA stage through a fiberized isolator which protected the seed source from back propagating power in the amplification stage, and hence ensured the stability of the seed source. The fiberized isolator is polarization-sensitive with the insertion loss about 0.95 dB, and its fiber pigtail has a single-mode (SM) polarization-maintaining (PM) structure with a 9- $\mu\text{m}$  core and 125- $\mu\text{m}$  cladding (9/125). The pump laser of the amplification stage is a commercial continuous-wave laser diode operating at 793 nm, and its power was coupled into the amplification stage through a PM combiner (ITF) with a coupling efficiency of 87.5%. A 1.4-m long double-clad PM thulium-doped fiber laser with a 10/130 structure (Nufern) was utilized as the gain medium of the PA. Its length was chosen for the trade-off between reabsorption effect at seed laser wavelength and sufficient pump power absorption. A 0.5-m long SM PM passive fiber, with the same structure as the fiber pigtail of the isolator, was spliced to the thulium-doped fiber laser; this single-clad fiber acted to strip out the cladding light from double-clad thulium-doped fiber, providing a SM output of the amplification stage. Both the seed laser cavity and the amplification stage were mounted on the aluminum heat sink and cooled by forced air at room temperature.

The output from the PA was collimated with a fiberized collimator (AFR) which gave a beam radius of 1.5 mm and a vertical linear polarization. This fundamental wave (FW) beam was aligned with two silver mirror (M1, M2), and was focused into a commercial 5% doped MgO:PPLN crystal (HCP) using a lens with  $f=150$  mm; the fundamental beam waist at the center of the crystal was  $\omega \sim 80$   $\mu\text{m}$ . The measurement showed that about 87% of FW power was launched into the MgO:PPLN due to the propagating loss introduced by the alignment system. The MgO:PPLN is 48-mm long with multiple poling periods ranging from 28.5 to 31.5  $\mu\text{m}$ , and is housed in an oven with a temperature stability of  $\pm 0.1$   $^{\circ}\text{C}$ . The crystal faces have AR coating ( $R < 0.8\%$ ) for the SH wavelength, with high transmission ( $T > 99\%$ ) for the fundamental wavelength. Moreover, both crystal faces are angle ( $1^{\circ}$ ) polished for the sake of preventing parasitic process in the single-pass SHG, and its length is optimized to prevent serious de-phasing effect. A dichroic mirror (M3) was used to separate the SH output beam from unconverted FW.

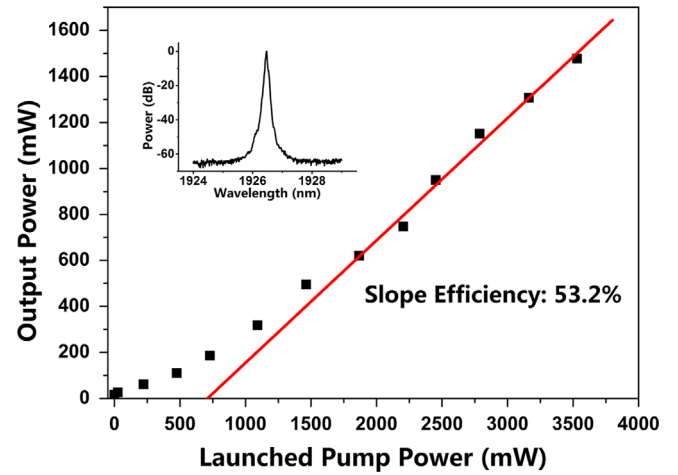


Fig. 2. The average output power versus launched pump power in the amplification stage. Inset: the spectrum of the output pulses from the amplification stage.

### 3. Results and theoretical model

The seed source of the system produced 45-ns pulses with average power of 700 mW at the repetition rate of 100 kHz. Linearly polarized output with average power about 595 mW was launched into the amplification stage, serving as the seed laser of the PA. There was an obvious power reduction in the seed laser when it passed through the PA without input 793-nm pump power; this was considered to be caused by the strong reabsorption effect of the thulium-doped fiber.

Fig. 2 illustrates the average power versus the launched pump power of the amplification stage. Initially, the seed power was not efficiently amplified due to the reabsorption effect; then the PA operated in the linear region when the launched pump power increased up to 1868 mW. The maximum average power produced from the PA was measured to be 1477 mW when a launched pump power was 3530 mW, with a slope efficiency of 53.2% in the linear region, which is higher than the value of 36% presented by Ref. [14]. The amplification efficiency of the PA was only 25% corresponding to a seed power of 595 mW, which was restricted by the reabsorption effect of the thulium-doped fiber and the upper limit of pump power. The power stability of the amplified output is similar to the performance of the seed laser mentioned in our previous work [12]. The spectrum of output pulses was measured by an optical spectrum analyzer (YOKOGAWA), and is

shown in the inset of Fig. 2; the 3 dB spectrum bandwidth (full width at half maximum, FWHM) of the amplified laser was 0.05 nm, centered in 1926.47 nm. It should be noticed that the pulse duration of the seed source, the center wavelength and the linewidth of output pulses from the PA were slightly different compared to our previous work [12]; these changes were probably attributed to day-to-day variations and a slight degradation in the MO of the seed laser because the fiber Bragg gratings used in the MO were written in the bare fiber without protection. The PER of the PA output was measured by propagating the pulses into a polarization analyzer. A PER more than 19.0 dB was achieved when the PA operated at all pump power levels, indicating that the FW beam for SHG was more than 98.7% linearly polarized at all conditions.

A theoretical model was employed in our experiment in order to analyze the SHG process based on MgO:PPLN. The model is derived from coupled-wave equations for SHG, and the Manley–Rowe relations are invoked [15]. In particular, we consider the MgO:PPLN as a lossless nonlinear optical medium involving collimated, monochromatic FW input beams. The efficiency  $\eta$  for conversion of power from the FW to the SHG, including the effect of wavevector mismatch, can be defined by

$$\eta = \frac{P_{SHG}}{P_{FW}} = \tanh^2 \left[ L \left( \frac{8\pi^2 d_Q^2}{n_{FW}^2 n_{SHG} \epsilon_0 c \lambda_{FW}^2} \cdot \frac{P_{FW}}{\pi \omega_0^2} \right)^{\frac{1}{2}} \right] \cdot \text{sinc}^2 \left( \frac{\Delta k \cdot L}{2} \right), \quad (1)$$

where  $P$  is peak power of SHG or FW,  $L$  is the length of the MgO:PPLN,  $n$  is the refractive index of SH or fundamental wavelength which are determined by temperature of the MgO:PPLN via the Sellmeier equation,  $\epsilon_0$  is the permittivity of free space,  $c$  is the speed of light in vacuum,  $\lambda_{FW}=1926.47$  nm is the fundamental wavelength in our case,  $\omega_0$  is the fundamental beam waist in the crystal. Since the MgO:PPLN is QPM material, a modified value of the nonlinear coupling coefficient  $d_Q$  is equal to the effective value  $d_{eff}$  reduced by a  $2/\pi$  factor; the  $d_{eff}$  is  $\sim 27$  pm/V for MgO:PPLN, and hence the  $d_Q$  is  $\sim 17.19$  pm/V. In addition, the wavevector mismatch for QPM material is given by

$$\Delta k = 2k_{FW} - k_{SHG} - \frac{2\pi}{\Lambda}, \quad (2)$$

where  $k$  is equal to  $2\pi n/\lambda$  at the SH or fundamental wavelength,  $\Lambda$  is the poling period of the MgO:PPLN. Maximum conversion efficiency in Eq. (1) can be achieved with the quasi-phase-matching condition  $\Delta k=0$ , thus the optimum period for the SHG

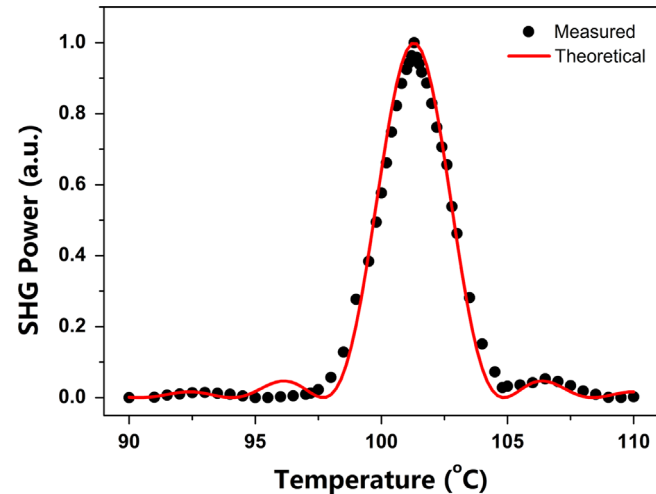


Fig. 3. The output power of the second-harmonic generation versus tuning temperature of the MgO:PPLN.

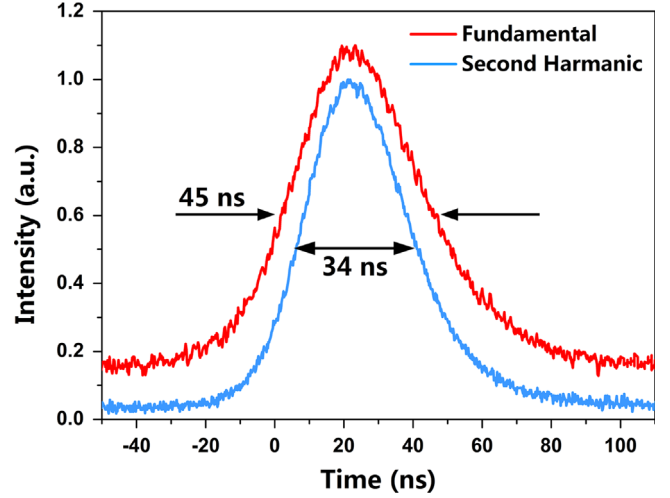


Fig. 4. The pulse durations of the fundamental wave and the second-harmonic generation.

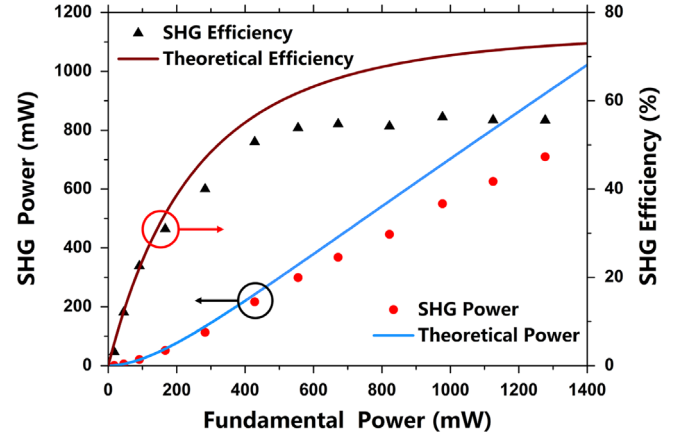


Fig. 5. The output power and the conversion efficiency of second-harmonic generation versus the launched power of the fundamental wave. (For interpretation of the references to color in this figure, the reader is referred to the web version of this article)

is given by

$$\Lambda = \frac{2\pi}{2k_{FW} - k_{SHG}}. \quad (3)$$

In our experiment, the poling period  $\Lambda=28.5$   $\mu\text{m}$  of the MgO:PPLN was chosen, and the optimal temperature of the crystal was calculated to be 101.3  $^{\circ}\text{C}$ .

There may be slight differences between the temperature seen by the beams and the setting temperature of the oven. Therefore, we investigated the optimal operating temperature of the MgO:PPLN when the launched FW power was 440 mW, with the results shown in Fig. 3. With temperature tuning from 90  $^{\circ}\text{C}$  to 110  $^{\circ}\text{C}$ , the SH output power was in good agreement with the theoretical curve derived by the model mentioned above. A maximum SH power was achieved at the temperature of 101.3  $^{\circ}\text{C}$ ; the temperature bandwidth (FWHM) for SHG was measured to be 3.1  $^{\circ}\text{C}$ . Therefore, the optimal temperature of 101.3  $^{\circ}\text{C}$  was selected in the SHG process, and typical pulse shapes of both FW and SHG were recorded (Fig. 4). As shown in Fig. 4, the pulse durations of the FW and the SHG were 45 ns and 34 ns, respectively. Both the FW and the SHG pulses maintained a Gaussian shape, and their mode-beating characteristics might be attributed to slight instability of the seed source.

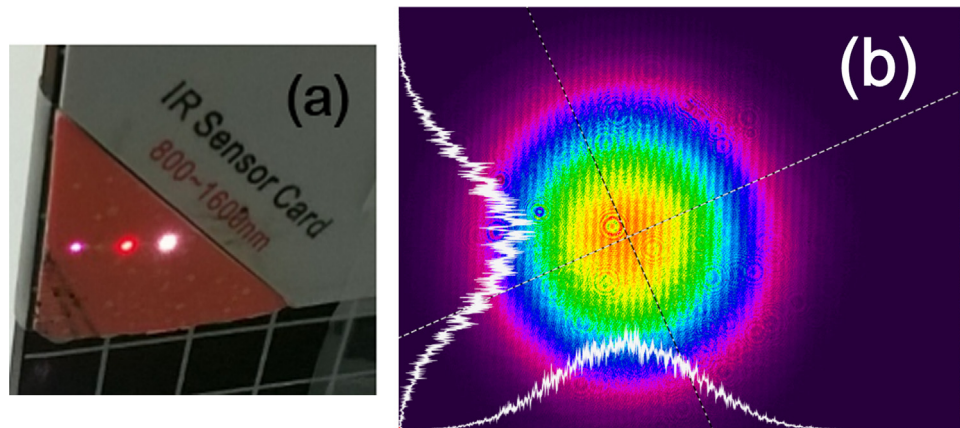


**Fig. 6.** (a) The separated spots of SHG, third- and fourth harmonic generations (from right to left). (b) The beam profile of the second-harmonic output. (For interpretation of the references to color in this figure, the reader is referred to the web version of this article)

The SHG output power and the SHG conversion efficiency versus the FW launched power are shown in Fig. 5; the theoretical curves derived by Eq. (1) are also included. The maximum SHG power of 710 mW at 963 nm was achieved, with up to 56% frequency doubling efficiency. According to 1550-nm pump power of 1960 mW in the seed source and 793-nm pump power of 3530 mW in the PA, the total optic-to-optic conversion efficiency for 963 nm generation was more than 12.9%. Moreover, unexpected red and blue light, corresponding to the third- and fourth-harmonic generations could be observed when the launched FW power increased up to 250 mW. These effects might be probably caused by the large nonlinearity ( $d_Q \sim 17.19$  pm/V) and the long interaction length (50 mm) of the MgO:PPLN crystal [13]. The dichroic mirror (M3) was replaced by a prism which was used to separate beams with different wavelengths in our experiment; the separated spots are shown in Fig. 6(a). With the maximum input FW power, the output power of the third- and fourth-harmonic generations was measured to be 2.74 mW and 3.23 mW, respectively.

As shown in Fig. 5, the measured SHG power was consistent with the theoretical curve until the launched FW power was higher than 220 mW, and hence the same tendency occurred in the SHG conversion efficiency. Several factors might lead to the discrepancy between the recorded data and theoretical curve. First, the third- and fourth-harmonics mentioned above were not included in the theoretical model. Part of the FW power was depleted by these effects, which resulted in the reduction of conversion efficiency for SHG process; the output power of these nonlinear processes grew larger when the FW power increased which led to further discrepancy between the measured power and the theoretical curve. In addition, the launched FW beam was not perfectly polarized, and thus only a beam in appropriate polarization orientation was useful for SHG. The imperfect AR coating of MgO:PPLN crystal surfaces would also lead to a slight reduction of the input FW power. Third, the FW beam waist was set to be a constant value in the theoretical model, whereas the FW had a Gaussian intensity profile. A constant compromise value  $\omega_0 = 102$   $\mu\text{m}$  of the FW beam waist was chosen in Eq. (1) since the beam waist in the center of the crystal was  $\omega_1 \sim 80$   $\mu\text{m}$  and the beam waist in the surface of the crystal was  $\omega_2 \sim 120$   $\mu\text{m}$ , and hence the angular divergence of the FW beam led to a reasonable mismatch between the measured data and the theoretical curve. Moreover, due to the long MgO:PPLN crystal, the back-conversion and thermal de-phasing effects in the MgO:PPLN crystal might also contribute to the discrepancy. Despite these unavoidable effects, the measured SHG power followed the approximate tendency with the theoretical model.

The measured far-field energy distribution of the SHG beam at 963 nm is presented in Fig. 6(b). The interference fringes on the color beam plot were probably ascribed to the attenuator which

was utilized to reduce SHG intensity in order to protect the CCD in beam profiler. Despite the interference, the beam profile of the SHG maintained a clear Gaussian distribution.

#### 4. Conclusion

In summary, we have demonstrated efficient 963 nm generation by frequency doubling a polarized TDFL system with MgO:PPLN. The SH process generates 34-ns pulses with average power up to 710 mW at a repetition rate of 100 kHz, which is in a good agreement with our theoretical model. The SH conversion efficiency of 56% and the total optic-to-optic conversion efficiency more than 12.9% have been achieved. Moreover, the third- and fourth harmonic generation from the TDFL have been observed in our experiments, indicating potential efficient operations of these nonlinear processes from TDFLs.

#### Acknowledgments

The authors would like to acknowledge Advanced Fiber Resources (Zhuhai) Ltd. for the technical support in this work. Special thanks to Dingxiang Cao, Deping Zhao and Qian Fu for helpful discussion. This work was partially supported by the National Natural Science Foundation of China under grants 61308056, 61008025, 11232015, 11072271 and 11204044, the Research Fund for the Doctoral Program of Higher Education of China under grants 20120171110005 and 20130171130003, the Project Supported by Guangdong Natural Science Foundation, China under grant S2012010010172, and the Opening Project of Science and Technology on Reliability Physics and Application Technology of Electronic Component Laboratory under grant ZHD201203.

#### References

- [1] Chu Z, Wilkerson TD, Singh UN. Water-vapor absorption line measurements in the 940-nm band by using a Raman-shifted dye laser. *Appl Opt* 1993;32(6):992–8.
- [2] Chr T, Schnier D. A tunable three-level neodymium-doped fiber laser and its application to depletion of the  $4f^{14} 5d 2D^{3/2}$  level in optically excited, trapped ytterbium ions. *Opt Commun* 1992;87(5):240–4.
- [3] Wassermann EF, Thielen M, Kirsch S, Pollmann A, Weinforth H, Carl A. Fabrication of large scale periodic magnetic nanostructures. *J Appl Phys* 1998;83(3):1753–7.
- [4] Zhang J, Ostroverkhov V, Singer KD, Reshetnyak V, Reznikov Y. Electrically controlled surface diffraction gratings in nematic liquid crystals. *Opt Lett* 2000;25(6):414–6.



- [5] Röser F, Jauregui C, Limpert J, Tünnermann A. 94 W 980 nm high brightness Yb-doped fiber laser. *Opt Express* 2008;16(22):17310–8.
- [6] Soh DBS, Seongwoo Y, Nilsson J, Sahu JK, Kyunghwan O, Seungin B, et al. Neodymium-doped cladding-pumped aluminosilicate fiber laser tunable in the 0.9- $\mu$ m wavelength range. *IEEE J Quantum Electron* 2004;40(9):1275–82.
- [7] Wang A, George AK, Knight JC. Three-level neodymium fiber laser incorporating photonic bandgap fiber. *Opt Lett* 2006;31(10):1388–90.
- [8] Clarkson WA, Barnes NP, Turner PW, Nilsson J, Hanna DC. High-power cladding-pumped Tm-doped silica fiber laser with wavelength tuning from 1860 to 2090 nm. *Opt Lett* 2002;27(22):1989–91.
- [9] Jiang M, Tayebati P. Stable 10 ns, kilowatt peak-power pulse generation from a gain-switched Tm-doped fiber laser. *Opt Lett* 2007;32(13):1797–9.
- [10] Willis C. C. C., Shah L., Baudelet M., Kadwani P., McComb T. S., Sims R. A., et al., High-energy Q-switched Tm<sup>3+</sup>-doped polarization maintaining silica fiber laser. In: *Proceedings of the International Society for Optics and Photonics (SPIE LASE)*, (2010). 758003-1–758003-6.
- [11] Simakov N, Hemming A, Bennetts S, Haub J. Efficient, polarised, gain-switched operation of a Tm-doped fiber laser. *Opt Express* 2011;19(16):14949–54.
- [12] Jiao Zhongxing, Zhang Baofu, Wang Biao. An all-fiber, polarized, core-pumped heat-resistant thulium-doped master oscillator power amplifier. *Laser Phys* 2013;23(8):085101.
- [13] Myers LE, Eckardt RC, Fejer MM, Byer RL, Bosenberg WR, Pierce JW. Quasi-phase-matched optical parametric oscillators in bulk periodically poled LiNbO<sub>3</sub>. *J Opt Soc Am B* 1995;12(11):2102–16.
- [14] Frith G, McComb T, Samson B, Torruellas W, Dennis M, Carter A, Khitrov V, Tankala K. Frequency doubling of Tm-doped fiber lasers for efficient 950nm generation. *Advance Solid-State Photonics (Optical Society of America)*. 2009.
- [15] Boyd Robert W. *Nonlinear Optics*. 3rd ed.. New York: Academic Press; 2008.